

# Recurrent and non-recurrent trajectories in a chaotic system



**A. B. Adeloje, A. O. Akala**

Physics Department, University of Lagos, Akoka-Yaba, Lagos, Nigeria.

**E-mail:** aadeloje@unilag.edu.ng; adeloyeab@yahoo.com

(Received 2 June 2010; accepted 6 August 2010)

## Abstract

The dynamics of a system subjected to a potential equal to the sum of the Henon-Heiles potential and that of the hydrogen atom in a uniform magnetic field has been studied. Depending on the energy of the system, the Poincare surface is characterised by regions of regular motion, appearing and disappearing regions of regular motion, regions of recurrent (regular and chaotic) trajectories and those of non-recurrent trajectories.

**Keywords:** Poincare surface, Recurrent and Non-recurrent trajectories, Coupled potential

## Resumen

Se ha estudiado la dinámica de un sistema sometido a un potencial igual a la suma del potencial Henon Heiles-y el del átomo de hidrógeno en un campo magnético uniforme. Dependiendo de la energía del sistema, la superficie de Poincaré se caracteriza por regiones de movimiento regular, apareciendo y desapareciendo regiones de movimiento regular, trayectorias de regiones recurrentes (regulares y caóticas) y de las trayectorias no periódicas.

**Palabras clave:** Superficie de Poincare, trayectorias recurrentes and non-recurrentes, potencial acoplado.

**PACS:** 02.30.Hq, 05.45.-a, 05.45.Pq

**ISSN 1870-9095**

## I. INTRODUCTION

The Henon-Heiles potential has played a prominent role in the development of the chaos theory. Suggested by Henon and Heiles [1] as the simplest potential that would produce all the complexities obtainable in any chaotic system, the potential has received a lot of attention from researchers, and has recently [2] been referred to as the most famous open Hamiltonian system.

The Henon-Heiles potential is given as

$$V(q_1, q_2) = \frac{q_1^2 + q_2^2}{2} + q_1^2 q_2 - \frac{1}{3} q_2^3, \quad (1)$$

Where  $q_i$  is the coordinate of the  $i$  th oscillator, with a corresponding momentum  $p_i$ ;  $i = 1, 2$ .

The modified form

$$V(q_1, q_2) = \frac{q_1^2 - q_2^2}{2} - q_1^2 q_2 + \frac{1}{3} q_2^3, \quad (2)$$

describing the motion of free test particles in vacuum gravitational pp-wave space-time has been studied by Vesely and Podolsky [3]. This is just different from the modified Henon-Heiles system studied by Choudhury and Kalita [4]:

$$V(q_1, q_2) = \frac{q_1^2 - q_2^2}{2} + \frac{1}{3} q_1^3 - q_1 q_2^2.$$

In addition, Brack, *et al.* [5] carried out an investigation of the modified Henon-Heiles potential,

$$V(q_1, q_2) = \frac{q_1^2 + q_2^2}{2} + \alpha \left( q_1^2 q_2 - \frac{1}{3} q_2^3 \right), \quad (4)$$

where  $\alpha$  is a coupling parameter.

The quartic Henon-Heiles potential has been investigated by Brack, *et al.* [5, 6]. The same problem was treated by Brack [7] in scaled coordinates as

$$V(q_1, q_2) = \frac{q_1^2 + q_2^2}{2} + \frac{3}{2} q_1^2 q_2^2 - \frac{1}{3} q_2^3. \quad (5)$$

The hydrogen atom has received a lot attention from researchers, ranging from the classical electronic motion of the atom near a metal surface [8], hydrogen atom in the presence of uniform magnetic and quadrupolar electric fields [9] to the hydrogen atom in parallel electric and magnetic fields [10].

We consider the hydrogen atom in a uniform magnetic field (of strength  $B$ ) described by the Hamiltonian [11]:

$$H = \frac{p^2}{2m_e} - \frac{e^2}{r} + \omega l_z + \frac{1}{2} m_e \omega^2 (x^2 + y^2)$$

where  $z$  is the direction of the field,  $m_e$  is the reduced mass of the electron and the nucleus, and  $\omega$  is half the cyclotron frequency, equal to  $\frac{eB}{2m_e c}$ . It has been shown that the

dynamics is equivalent to that given by the Hamiltonian [11]:

$$H_0(q_1, q_2, p_1, p_2) = \frac{1}{2} p_1^2 + p_2^2, -s q_1^2 + q_2^2 + \frac{1}{8} q_1^2 q_2^2 q_1^2 + q_2^2, \quad (7)$$

where the scaled energy,  $s = \frac{B}{B_0} = \frac{\hbar\omega}{\mathfrak{R}}$ , determines the

degree of chaoticity of the system and  $B_0 = m_e e^3 c / h^3$ , the value of the magnetic field strength at which the oscillator energy equals the Rydberg energy,  $\mathfrak{R}$ .  $q_1, p_1, q_2$  and  $p_2$  are the coordinates and momenta of the equivalent system. The last term in Eq. (7) is the diamagnetic coupling term.

The system described by Eq. (7) has been studied extensively and found to be fully chaotic for  $s = -1.0$  [11].

## II. METHODOLOGY

In this work, the potentials of the two systems discussed above are coupled, that is,

$$V_1 = \left( \frac{q_1^2 + q_2^2}{2} \right) + q_1^2 q_2^2 - \frac{1}{3} q_2^3,$$

and

$$V_2 = \frac{1}{8} q_1^2 q_2^2 q_1^2 + q_2^2 - s q_1^2 + q_2^2,$$

to obtain

$$V = V_1 + V_2 = \left( \frac{q_1^2 + q_2^2}{2} \right) + q_1^2 q_2^2 - \frac{1}{3} q_2^3 +$$

$$\frac{5}{2} q_1^2 q_2^2 q_1^2 + q_2^2 - s q_1^2 + q_2^2,$$

where the diamagnetic coupling term has a factor of  $\frac{5}{2}$ , and not  $\frac{1}{8}$ .

With the potential, the Hamiltonian governing the motion of the oscillators is given as,

$$H = \left( \frac{p_1^2 + p_2^2}{2} \right) + \left( \frac{q_1^2 + q_2^2}{2} \right) + q_1^2 q_2^2 - \frac{1}{3} q_2^3 + \frac{5}{2} q_1^2 q_2^2 q_1^2 + q_2^2 - s q_1^2 + q_2^2. \quad (8)$$

The resulting equations of motion are given by

$$\frac{dp_i}{dt} = -\frac{\partial H}{\partial q_i}, \quad i = 1, 2, \quad (9)$$

$$\frac{dq_i}{dt} = +\frac{\partial H}{\partial p_i}, \quad i = 1, 2. \quad (10)$$

The equations to be solved, therefore, are:

$$\frac{d}{dt} p_1 = -\frac{\partial H}{\partial q_1}, = -[(1-2s)q_1 + 2q_1 q_2^2 + 5q_1 q_2^2 (2q_1^2 + q_2^2)], \quad (11)$$

$$\frac{d}{dt} p_2 = -\frac{\partial H}{\partial q_2}, = -[(1-2s)q_2 + q_1^2 + 5q_1^2 q_2 (q_1^2 + 2q_2^2) - q_2^2] \quad (12)$$

$$\frac{dq_1}{dt} = p_1, \quad (13)$$

$$\frac{dq_2}{dt} = p_2. \quad (14)$$

With the energy,  $E$ , ranging from 0.51 to 1.1, the Poincare surface has been investigated with a view to determining the area of the phase space covered by invariant curves.

The equations were solved using the Runge-Kutta fourth order method, and the Poincare surface of section determined by  $q_1 = 0, p_1 > 0$ . This reduced the phase space to a two dimensional subspace, the Poincare surface of section. The trajectory can intersect the Poincare surface either way, but by requiring that  $p_1 > 0$ , intersections in only one direction are studied.

### III. RESULTS AND DISCUSSION

Figures 1 and 2 show the Poincare surface of section of the system under consideration. In Fig. 1a, the gaps between the three major regions, the horizontally opposite (regular) regions, and the central region consists of non-recurrent trajectories. The central region encloses elliptic orbits. An initial point in the gaps leaves the Poincare surface after just a few intersections. This behaviour continues until energy equals 0.55 (Fig. 1b), where it is evident that the elliptic region around (0, 2) is about to break away from the rest of this particular region. In addition, the central region itself is now clearly not an island. The detachment is complete when the energy is 0.56 (Fig. 1c). In Fig. 1d, the portion that separated from the main central region becomes more chaotic when the energy increases to 0.58. However, there is yet a transition, of the breakaway central region, to a less chaotic situation between 0.58 and 0.6, as is evident from Fig. 1e. Increasing the energy to 0.62 ensures that the whole of the central region becomes more chaotic, including the breakaway part, which still retains an elliptic region (Fig. 1f). Moreover, the inner part of the main central region breaks into three regions of regular motion. In addition, the horizontally opposite regular regions have become chaotic. These two regions have become non-recurrent by energy 0.65, as only the three regular regions within the main central region, as well as the diminished regular region in the breakaway region remains (Fig. 1g). The latter regular region diminishes further through the value of energy 0.68 (Fig. 1h), after which it joins the non-recurrent region. As the energy increases to 0.74, the upper and lower regions of the central region become more chaotic, leaving the smaller regular regions (Fig. 2a). These chaotic regions increase at the expense of the regular regions until energy 0.8 (Fig. 2b). Yet again, there is a transition to a less chaotic situation in these opposite regions as evident in Fig. 2c, when the energy is 0.84. At this energy, the central regular region has the boundary encroaching on it. Increasing the energy further results in Fig. 2d (energy 0.88), where the regular region in the centre of the figure has been narrowed down considerably by the surrounding chaotic sea. However, the central region remains through energy 0.92 (Fig. 2e) to energy 1.0 (Fig. 2f), as well as the oppositely located regular regions, which are now even much smaller. By energy 1.05 (Fig. 2g), the central regular region has disintegrated. Indeed, the points shown in the centre of the figure are non-recurrent. By 1.1 (Fig. 2h), no recurrent trajectory exists. The points shown in Fig. 1.1 are indeed what is left of the two horizontally opposite regular regions, and the points shown are a part of non-recurrent trajectories.

### IV. CONCLUSION

An investigation of the sum of the potentials due to Henon-Heile and that of the hydrogen atom in an uniform magnetic field between the energies 0.51 and 1.1 gives rise

to regular, chaotic, recurrent and non-recurrent behaviour, depending on the energy, with more than one of these phenomena present at all values of the energy. Even at the lowest limit of the energy range considered, parts of the Poincare surface consist of non-recurrent trajectories. As the energy increases, the elliptic regions, elliptic regions break up into chaotic regions, which in turn become regions of non-recurrence. It is also noted that some regions make a transition from regular to chaotic and then become less chaotic, with regular regions appearing within them. At the higher energies, all the regular regions and the chaotic ones become non-recurrent, so that beyond a certain energy (equal to 1.1), the entire Poincare surface is devoid of recurrent orbits.

### REFERENCES

- [1] Henon, M., Heiles, C. *The Applicability of the Third Integral of Motion: Some Numerical Experiments*, The Astronomical Journal **69**, 73-79 (1964).
- [2] Barrio, R., Blesa, F., Serrano, S. *Bifurcations and safe regions in open Hamiltonians*, New J. Phys. **11** (2009), 053004.
- [3] Vesely, S., Podolsky, R. *Chaos in a modified Henon-Heiles system describing Geodesics in Gravitational Waves*, Phys. Lett. A **271**, 368-376 (2000).
- [4] Choudhury, B. K. D., Kalita, B. C. *Studies On Curvature Tensor and Geodesic Deviation Equation*, Proceedings of the 30th International Cosmic Ray Conference. July 3 - 11, 2007, Mérida, Yucatán, Mexico. Edited by Rogelio Caballero, Juan Carlos D'Olivo, Gustavo Medina-Tanco, Lukas Nellen, Federico A. Sánchez, José F. Valdés-Galicia. Universidad Nacional Autónoma de México, Mexico City, Mexico, Vol. 3, 1279-1282 (2008).
- [5] Brack, M., Meier, P., Tanaka, K. *Uniform trace formulae for SU(2) and SO(3) symmetry breaking*, J. Phys. A **32**, 331-353 (1999).
- [6] Brack, M., Creagh, S. C., Law, J. *Level density fluctuations at the bottom of a potential*, Phys. Rev. A **57**, 788-797 (1998).
- [7] Brack, M. *Bifurcation cascades and self-similarity of periodic orbits with analytical scaling constants in Henon-Heiles type potentials*, Found. Phys. **31**, 209-232 (2001).
- [8] Simonovic, N. S. *Classical Chaos in the Hydrogen Atom near a metal surface*, J. Phys. B: At., Mol. Opt. Phys. **30**, L613-L618 (1997).
- [9] Inarrea, M., Salas, J. P. *Hydrogen Atom in the presence of uniform magnetic and quadrupolar electric fields: Integrability, bifurcation, and chaotic behaviour*, Phys. Rev. E **66**, 056614 (2002).
- [10] Delande, D., Zakrzewski, J. *Experimentally attainable example of Chaotic Tunnelling: The Hydrogen Atom in Parallel Electric and Magnetic Fields*, Phys. Rev. A **68**, 062110 (2003).
- [11] Friedrich, H., Wintgen, D. *The Hydrogen Atom in a Uniform Magnetic Field – An example of Chaos*, Phys. Rep. **183**, 37-79 (1989).

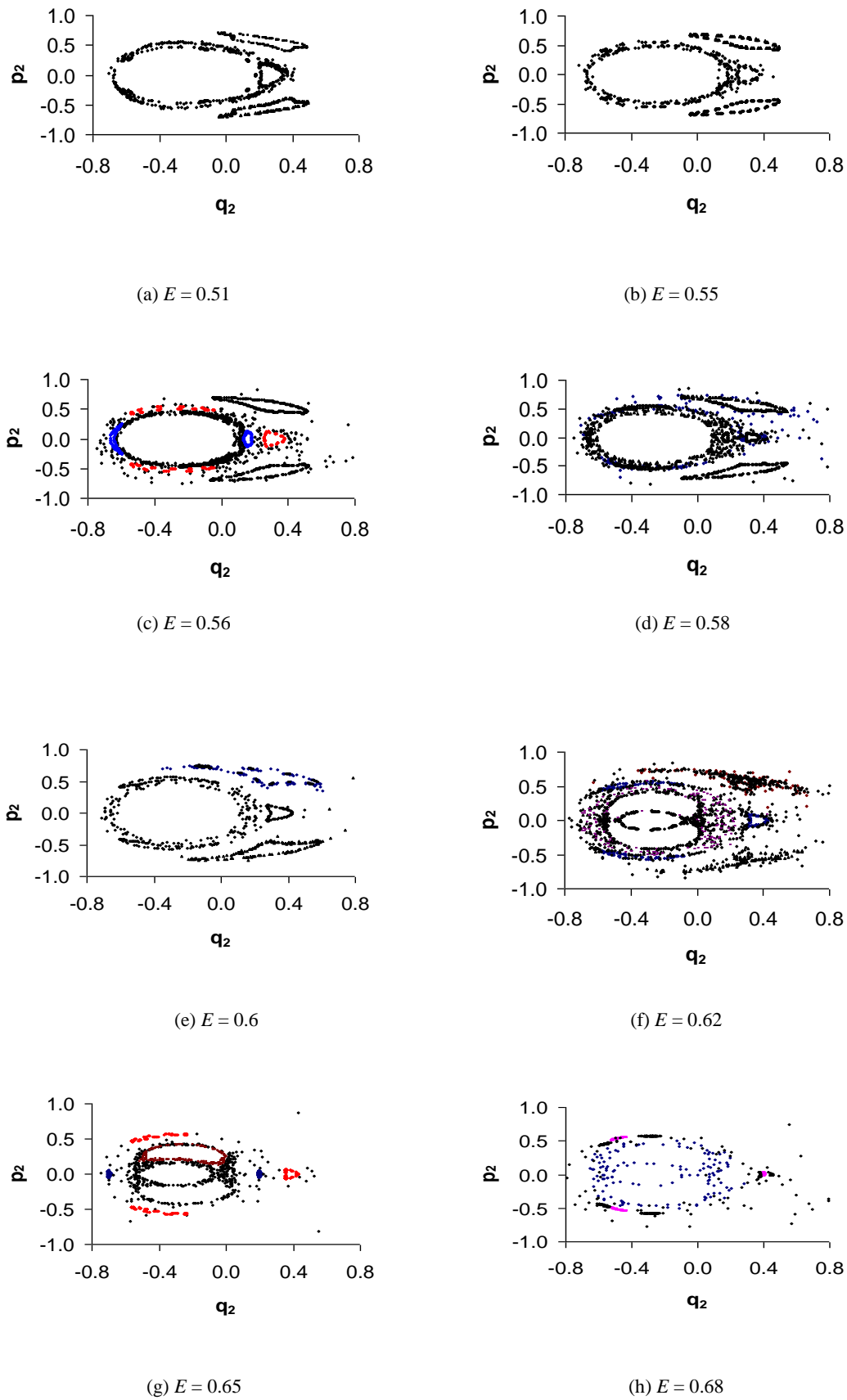


FIGURE 1. Poincaré surface of section for values of energy 0.51 to 0.68

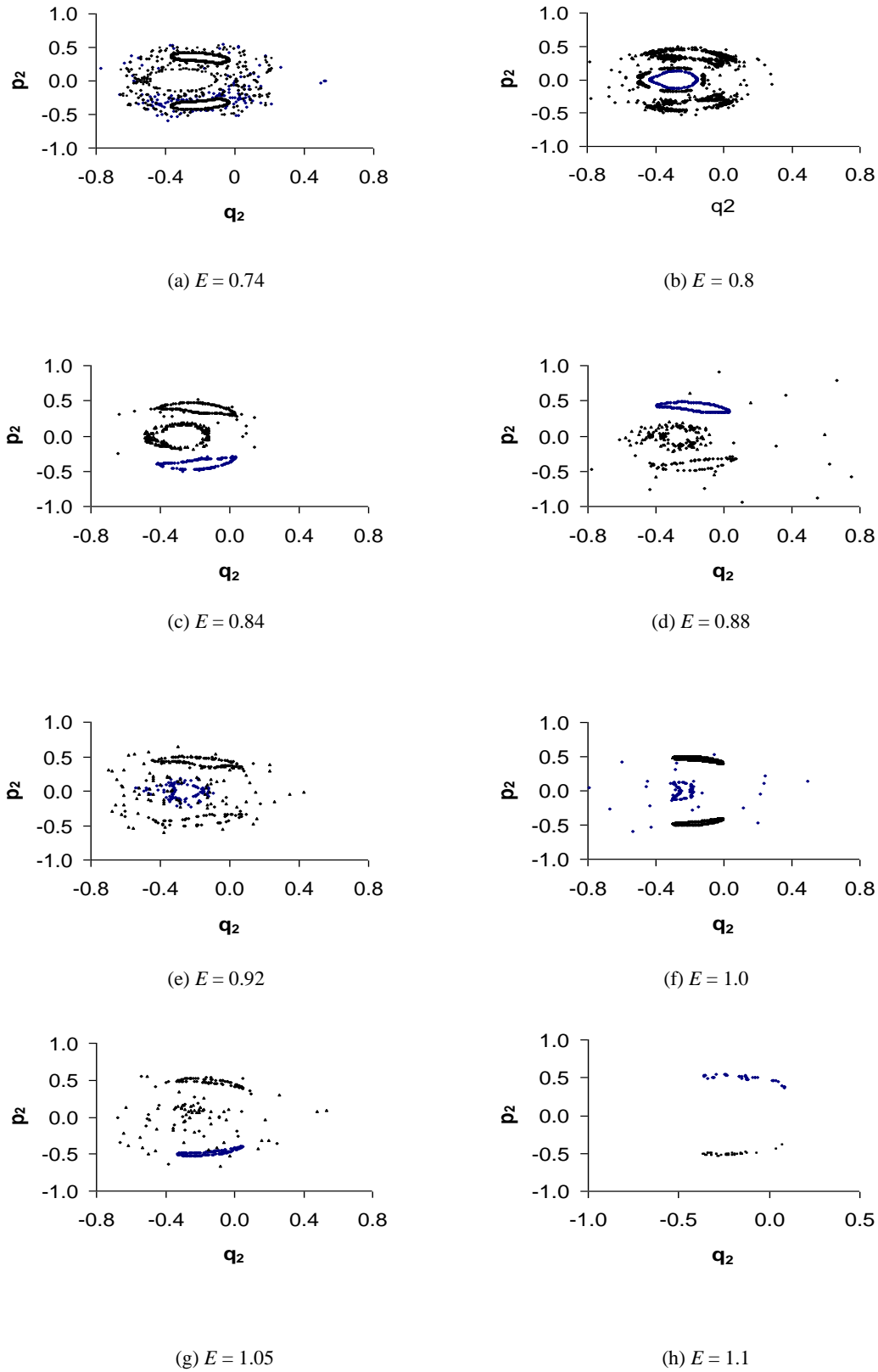


FIGURE 2. Poincaré surface of section for values of energy 0.74 to 1.1